Brain Advance Access published May 23, 2007

doi:10.1093/brain/awm102 *Brain* (2007) Page 1 of 10

Diffusion tensor imaging in preclinical and presymptomatic carriers of familial Alzheimer's disease mutations

John M. Ringman,[1] Joseph O'Neill,[2] Daniel Geschwind,[1] Luis Medina,[1] Liana G. Apostolova,[1] Yaneth Rodriguez,[3] Barbara Schaffer,[1] Arousiak Varpetian,[4] Benjamin Tseng,[5] Freddy Ortiz,[1,6,7] Jaime Fitten,[1,6,7] Jeffrey L. Cummings[1,2] and George Bartzokis[1,8]

[1]Alzheimer's Disease Research Center, UCLA Department of Neurology, Los Angeles, CA, [2]Psychiatry and Biobehavioral Science, UCLA, Los Angeles, CA, USA, [3]Laboratory of Experimental Psychology, National Institute of Neurology and Neurosurgery, Mexico City, Mexico, [4]Department of Neurology, Keck School of Medicine, USC, Rancho Los Amigos National Rehabilitation Center, Downey, CA, [5]Ahmanson-Lovelace Brain Mapping Center, UCLA, Los Angeles, CA, [6]Neuropsychiatry Research Memory Clinic, Olive View-UCLA Medical Center, Sylmar, CA, USA, [7]Greater Los Angeles Veterans Affairs Healthcare System, Sepulveda Campus and [8]Department of Psychiatry, VA Greater Los Angeles Healthcare System, West Los Angeles, California, USA

Correspondence to: John M. Ringman, MD, Assistant Professor, UCLA Department of Neurology, Alzheimer's Disease Research Center, 10911 Weyburn Ave, Suite 200, Los Angeles, CA 90095-7226, USA
Email: jringman@mednet.ucla.edu

Measures are needed that identify persons that will develop Alzheimer's disease in order to target them for preventative interventions. There is evidence from animal, pathological and imaging studies that disruption of white matter occurs in the course of Alzheimer's disease and may be an early event. Prior studies have suggested that late-myelinating regions or white matter connecting limbic structures are particularly susceptible to degradation. Persons destined to develop the disease by virtue of fully penetrant genetic alterations (familial Alzheimer's disease or FAD) provide a model in which early and even presymptomatic changes of the disease may be identified. In this study we performed diffusion tensor imaging (DTI) on 2 demented and 21 subjects at-risk for inheriting an FAD mutation. We compared global and localized fractional anisotropy (FA) measures in white matter between FAD mutation carriers and non-carriers in the preclinical (clinical dementia rating <1, $n = 20$) and presymptomatic (clinical dementia rating = 0, $n = 15$) stages of the disease. There were no significant differences between mutation carriers and non-carriers with regard to absolute age, age relative to the typical age of disease diagnosis in their family, gender or Mini-Mental Status Examination Score. Among preclinical FAD mutation carriers ($n = 12$), mean whole brain white-matter FA ($P = 0.045$), FA of the columns of the fornix ($P = 0.012$), area of the perforant pathways bilaterally (right side: $P = 0.028$, left side: $P = 0.027$) and left orbitofrontal lobe ($P = 0.024$) were decreased relative to that of non-carriers ($n = 8$). We also found that FA in the columns of the fornix ($P = 0.008$) and left orbitofrontal lobe white matter ($P = 0.045$) were decreased in the eight presymptomatic mutation carriers compared to seven non-carriers. Logistic regression demonstrated that FA of the columns of the fornix was a better predictor of mutation status than was cross-sectional area of the fornix, global mean white-matter FA and left frontal lobe white-matter FA. In a linear regression analysis, white-matter volume ($P = 0.002$), hippocampal volume ($P = 0.023$) and mutation status ($P = 0.032$) significantly predicted fornix FA. We conclude that FA is decreased in the white matter in preclinical and even presymptomatic FAD mutation carriers, particularly in the late-myelinating tracts connecting limbic structures. Decreased FA in of the columns of the fornix is particularly robust in early FAD and may provide a biomarker for early disease in sporadic Alzheimer's disease.

Keywords: familial Alzheimer's disease; presymptomatic; diffusion tensor imaging; fractional anisotropy; Presenilin-1; amyloid precursor protein; white matter; fornix; biomarker

Abbreviations: APP = amyloid precursor protein; CDR = clinical dementia rating; DTI = diffusion tensor imaging; DWI = diffusion-weighted imaging; FAD familial Alzheimer's disease; MCI = mild cognitive impairment

Received December 15, 2006. Revised March 26, 2007. Accepted April 5, 2007

Introduction

Disruption of white matter in Alzheimer's disease has been demonstrated in studies of post-mortem human brain (Chia *et al.*, 1984; Englund *et al.*, 1988), in animal models (Pak *et al.*, 2003; Wirths *et al.*, 2006) and *in vivo* in humans (Bartzokis *et al.*, 2003, 2004). The electron microscopic appearance of white matter in Alzheimer's disease was described in 1964 (Terry *et al.*, 1964). In this report, the normal lamellar structure of myelin was noted to be lost in places despite relatively normal-appearing axoplasm. It has been argued that such disruption of white matter reflects the susceptibility of late-myelinating regions to the effects of aging and Alzheimer's disease, and that these changes are primary in causing the clinical manifestations of the disease (Bartzokis, 2004). Whether a primary or secondary event in the aetiology of Alzheimer's disease, a comprehensive explanation of the disease must include an understanding of these changes.

Diffusion-weighted imaging (DWI) takes advantage of the ability of MRI to measure the direction and magnitude of proton diffusion. Various measures of water proton diffusion can be obtained using DWI including the overall magnitude of diffusion (diffusivity) as well as the tendency with which diffusion tends to be directionally dependent. This latter property is measured by calculating a diffusion tensor for each voxel using diffusion tensor imaging or DTI (Basser *et al.*, 1994). As diffusion in white matter tends to be parallel to the direction of fibre tracts and disruption of these tracks can reduce this tendency, DTI provides a measure of white-matter integrity. Fractional anisotropy (FA) is one index of the tendency for water diffusion to occur in a single direction within a voxel. FA is measured on a scale from 0 (random diffusion) to 1 (highly linear diffusion).

Previous studies of changes in white-matter integrity in Alzheimer's disease employing DTI have variably shown relatively increased mean diffusivity and decreased FA in anterior (Bozzali *et al.*, 2002) or posterior (Medina *et al.*, 2006) regions of white matter. Other DTI studies have attempted to elucidate the earliest point at which such changes can be detected by focusing on persons in the earliest clinical stages of the disease (mild cognitive impairment or MCI) or persons at genetic risk for Alzheimer's disease by virtue of carrying an ApoE ε4 allele. A recent study (Rose *et al.*, 2006) found increased diffusivity in the entorhinal and parieto-occipital cortices as well as other regions and decreased FA in the limbic parahippocampal sub-gyral white matter in persons with MCI compared to controls. Another study found that mean diffusivity in the hippocampus in persons with the amnestic sub-type of MCI predicted future progression to dementia (Kantarci *et al.*, 2005). The ApoE ε4 allele, which accounts for about 13% of ApoE alleles in the non-demented elderly caucasian population (Tang *et al.*, 1998), is the most important known genetic risk factor for the development of late-onset Alzheimer's disease. A DTI study demonstrated that non-demented carriers of the ApoE ε4 allele had lower FA in the corpus callosum (particularly in its posterior portion) and in the left posterior hippocampus relative to persons not carrying this allele (Persson *et al.*, 2006).

Though studying persons with MCI and those carrying the ApoE ε4 allele increase our ability to study the earliest stages of Alzheimer's disease, these factors are imperfect predictors of the future development of the disease. Identification of the earliest changes occurring in Alzheimer's disease therefore remains a challenge. Three genes have been identified, alteration of which causes a nearly 100% penetrant, autosomal dominantly inherited form of Alzheimer's disease. Though rare, the study of persons at-risk for inheriting this form of FAD due to mutations in the Presenilin-1 (PS1) or amyloid precursor protein (APP) genes provides a model in which we can use DTI to study white matter in persons in whom the future development of Alzheimer's disease can be reliably predicted. In the current study, we used DTI to quantify white-matter integrity in persons destined to develop Alzheimer's disease by virtue of inheriting mutations causing FAD. We hypothesized that FAD mutation carriers would have decreased FA in white-matter tracts connecting limbic structures (the cingula and columns of the fornix) and in late-myelinating regions (frontal lobe white matter and genu of the corpus callosum) as opposed to early-myelinating regions (inferior splenium of the corpus callosum and corticospinal tracts). We compared mean overall white-matter FA between preclinical (some cognitive impairment present but not demented) and presymptomatic (without identifiable cognitive deficits) FAD mutation carriers and non-carriers as well as FA in these specific areas.

Materials and methods

Population

Twenty-three persons established to have ($n = 2$) or be at-risk for ($n = 21$) known pathogenic PS1 ($n = 19$) or APP ($n = 4$) mutations received in-depth clinical, cognitive and imaging assessments. The Clinical Dementia Rating Scale (CDR) was performed by the PI and the Mini-Mental Status Examination (MMSE) by a research assistant. Both investigators performed these assessments blind to subjects' genetic status in 20 subjects. Mutation status had been clinically established in the two demented patients and one presymptomatic at-risk patient. At-risk persons who tested negative for the FAD mutation present in their family served as controls in this study. All subjects, or their

proxies, signed written, informed consent. All study procedures were approved by the Institutional Review Boards at UCLA and the National Institute of Neurology and Neurosurgery in Mexico City.

Magnetic resonance imaging

All images were obtained on the same 1.5 T Siemens Sonata MRI scanner. Four immediately sequential, six-direction diffusion-weighted whole-brain volumes were acquired on all subjects in the plane of the AC–PC line using Echo-Planar Imaging (EPI) with a TR of 6 s, TE of 78 ms. *B*-values were 0 and 1000 s/mm^2. Voxel size was $3 \times 3 \times 3\,\text{mm}^3$. FA maps were then generated using the FMRIB's Diffusion Toolbox (FDT) in FSL software (version 3.2) (Behrens *et al.*, 2003; Smith *et al.*, 2004). The four volumes for each subject were co-registered using FMRIB's Linear Image Registration Tool (FLIRT) to correct for any shift in head position between acquisitions (Jenkinson and Smith, 2001). These four volumes were then averaged together. The averaged $B = 1000\,\text{s/mm}^2$ volume generated six sub-volumes, each representing one of the six diffusion directions. These subvolumes together with the $B = 0$ (non-diffusion weighted) volume were concatenated into seven volumes in a single file. Eddy current correction was then applied, also using FDT. A diffusion tensor model was fit at each voxel using FDTs DTIFIT, generating fractional anisotropy (FA) maps. Two types of analyses were performed on these FA maps; global and region-of-interest (ROI) analyses of selected areas in white matter.

All subjects also underwent structural MRI in the same session as DTI. Whole-brain T1-weighted images were obtained in the sagital plane using an MP-RAGE sequence (TR = 1900 ms, TE = 4.38 ms, TI = 1100 ms, flip angle 15°). Voxel size was $1 \times 1 \times 1\,\text{mm}^3$. Brain volumes were extracted from the cranium and extracranial tissues using FMRIB's Brain Extraction Tool (Smith, 2002). Gray and white-matter volumes (normalized to total intracranial volume) were calculated using FMRIB's SIENAX (Structural Image Evaluation, using Normalisation, of Atrophy) (Smith *et al.*, 2002). Cross-sectional areas of the columns of the fornix were estimated for each subject using methods similar to Callen *et al.* (2001). Specifically, the axial slice in which the descending fornices were closest to each other and where the cross-sectional area appeared greatest was chosen and the cross-sectional area measured using FSLView (Fig. 1). Hippocampi were traced by the PI using FSLView according to the protocol of Pantel *et al.* (2000). Volumes were calculated using FSL software and normalized to intracranial volume. Normalized right and left hippocampal volumes were averaged for the multivariate analysis (see later).

For the global analyses of white matter, brain-extracted whole-brain volumes from T1-weighted images were registered to Talairach space using FLIRT. These registered volumes were segmented into CSF, white and gray matter using FMRIB's Automated Segmentation Tool (Zhang *et al.*, 2001). The FA maps created as above were then also registered to Talairach space using FLIRT. The white-matter volumes from the structural images were then used as masks to delineate the white-matter volumes from the FA maps for each subject (Fig. 2). Average FA values of white matter were then calculated for each subject from these white-matter FA maps.

For all ROI analyses other than the perforant pathway, voxels were selected from the FA maps in native space by two co-investigators blind to subjects' genetic or clinical status. Specifically, two voxels each representing the splenium and genu of the corpus callosum, the right and left corticospinal tracts at the level of the mesencephalon and bilateral frontal white matter were chosen by one investigator (GB). In regards to the anterior corpus callosum, we desired to obtain a sample that would consistently be in the middle of the structure in order to sample tracts connecting the prefrontal cortices. Therefore, voxels from the genu of the corpus callosum were chosen from the two axial slices on which the angle formed by the

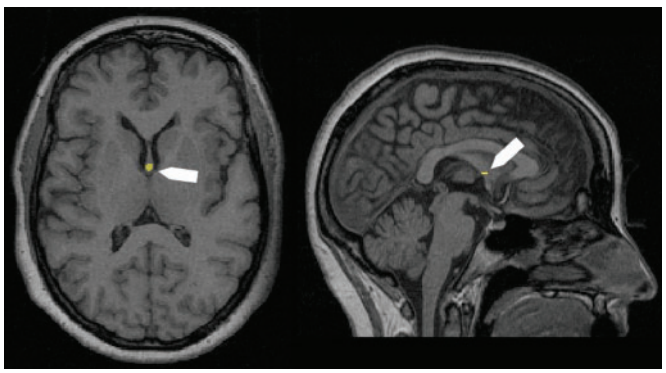

Fig. 1 Axial (left) and sagital (right) views of an exemplary image in which the descending columns of the fornix were localized, delineated and cross-sectional area calculated.

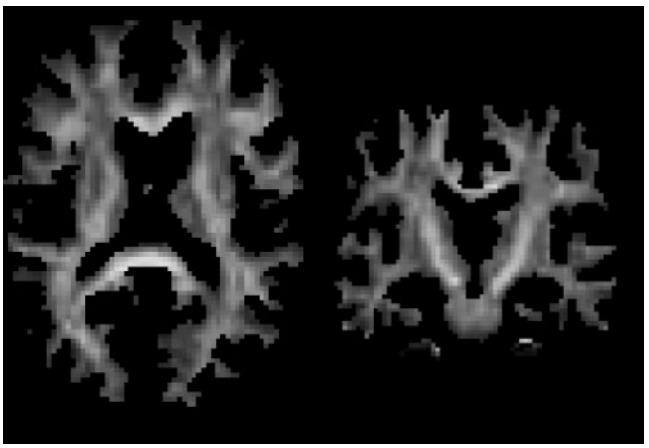

Fig. 2 Axial (left) and coronal (right) views of a Talairach-registered extracted white-matter FA map.

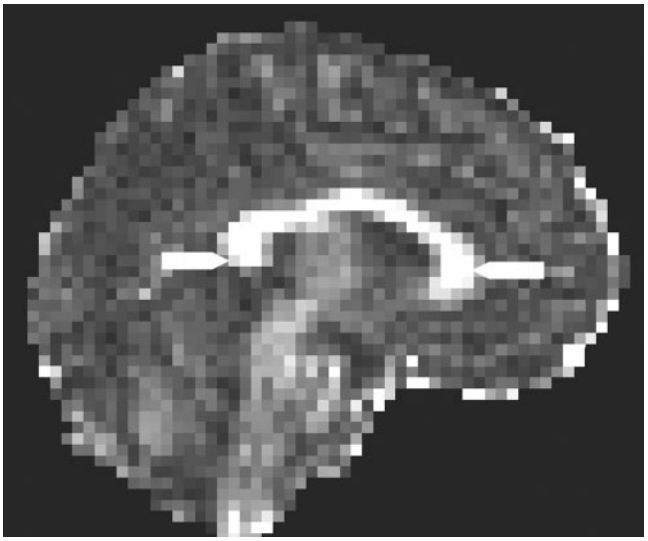

Fig. 3 Two contiguous corpus callosum voxels were chosen on both sides of the midline in the horizontal planes depicted by arrows. The plane of the genu (right) was defined by its widest part, where axons connecting the prefrontal cortices cross. The plane of the splenium was below its widest part, where axons connecting primary visual cortex cross.

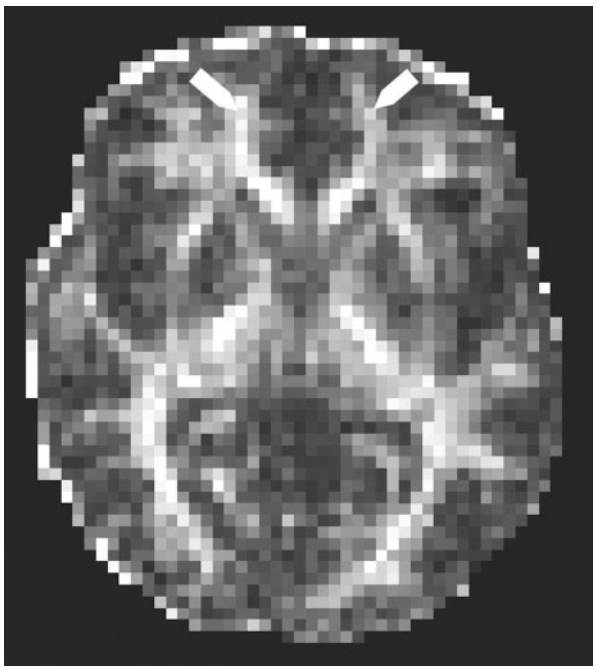

Fig. 4 Two contiguous voxels were chosen in the inferior frontal white matter where it is elongated in the anterior–posterior direction in a slice superior to the orbitofrontal cortex and inferior and slightly anterior to the cingulate gyrus.

left and right sides of the genu appeared the most linear (Fig. 3). For the splenium of the corpus callosum, the second and third lowest slices on which the fibres of the splenium connected in the midline were chosen in order to sample the lower half of the splenium which contains

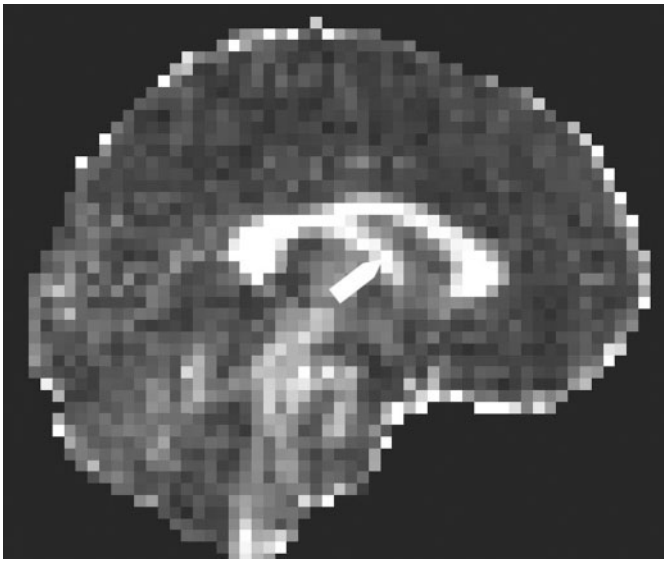

Fig. 5 Axial view of an exemplary FA map demonstrating how the brightest voxel corresponding to the descending columns of the fornix was chosen.

predominantly primary sensory (visual) fibres (Fig. 3, for details see Bartzokis *et al*., 2006). For both structures two pairs of adjacent voxels were used, one set to the left and one to the right of the structure midline. For analysis of frontal lobe white matter, the voxels chosen were anterior (towards the frontal pole) and superior to the orbitofrontal cortex. To ensure that gray matter was not included in the ROI, the gyrus rectus was identified and the two white-matter voxels chosen were superior to it and inferior and slightly anterior to the cingulate gyrus (i.e. where the frontal white matter still is elongated in the anterior–posterior direction, Fig. 4). For each hemisphere, the averages of the FA values of the two voxels in the splenium, genu and inferior frontal lobes were taken as representative for the respective region.

The brightest voxel corresponding to the body of the fornices, the right and left cingulum bundle and the area of the perforant pathway were chosen by another investigator (LA). Orthogonal views of the FA maps in native space were employed to pick the brightest voxel corresponding to the descending columns of the fornix (Fig. 5). Again in native space, FA colour maps in which the directionality of diffusion is colour-coded were generated and used to facilitate the selection of posterior cingulum voxels. Representative right and left posterior cingulum voxels were chosen as voxels having blue colour (i.e. preponderence of superior–inferior diffusion) located behind the corpus callosum (identified as a strip of red colour, i.e. preponderance of right–left diffusion). To define FA in the area of the perforant pathways, FA maps and T1-weighted images were co-registered in Talairach space. These images were superimposed and for each subject the sagital slice where the hippocampus was seen in its full length was used to select voxels in the underlying region of the perforant

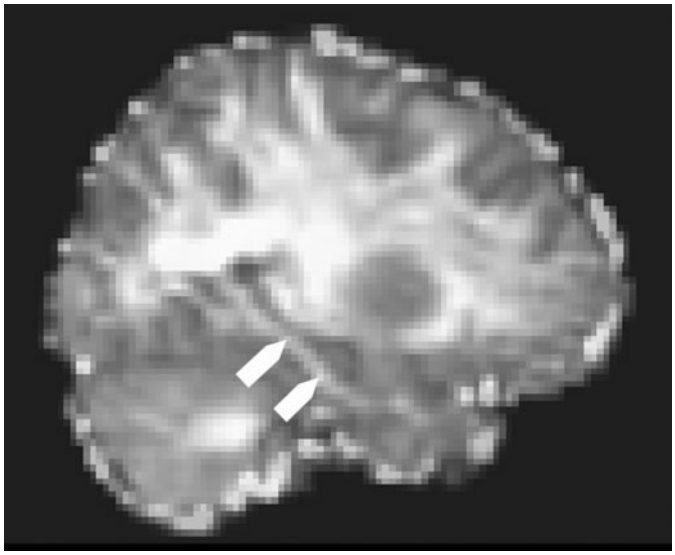

Fig. 6 Sagital view of superimposed Talairach-registered T1-weighted image and FA map depicting how voxels in the are of the perforant pathway were selected (see text for details).

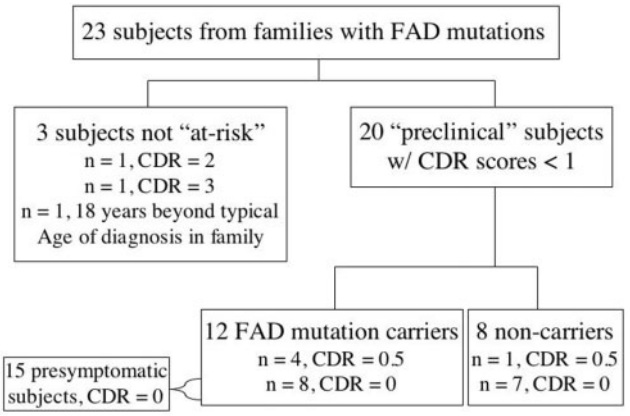

Fig. 7 Chart indicating the break-down of subjects by clinical and FAD mutation status. CDR = Clinical Dementia Rating scale.

pathway. Two voxels were chosen on each side: the brightest FA voxel underlying the head of the hippocampus (e.g. it's anterior third) and the brightest voxel underlying the anterior part of the body of the hippocampus (or it's middle third, Fig. 6). These were then averaged to provide the value for that side.

Genetic testing

Subjects underwent genetic testing for the FAD mutation for which they were known to be at-risk. They were informed they would be tested but in the context of the research protocol would not be told the result. The option of revealing genetic testing through a genetic counselor outside of the study was offered. Blood samples were coded according to a unique identifier and forwarded to the genetics laboratory. DNA was extracted and ApoE genotyping were performed using standard techniques. The presence of the A431E (number at risk = 11) and L235V ($n = 7$) substitutions in PSEN1 were assessed using RFLP analyses. The presence of the G206A substitution in PSEN1 ($n = 1$) and the V717I substitution in APP ($n = 4$) was assessed directly with bi-directional sequencing.

Statistical analyses

Subjects were categorized as either demented (CDR total scores ≥ 1), 'preclinical' (CDR scores <1) or 'presymptomatic' (CDR scores = 0). Within families harbouring PS1 and APP mutations, the age of disease onset tends to be fairly consistent (Fox *et al.*, 1997). Therefore, in order to estimate the subjects' age relative to the typical age of onset in their families, an 'adjusted age' or number of years prior to the typical age of dementia diagnosis in their families was calculated.

Table 1 Demographic data for the 12 preclinical (CDR total score <0.5) FAD MCs (mutation carriers) and 8 non-carriers (NCs)

	FAD MCs ($n = 12$)	FAD NCs ($n = 8$)	*P*-values
Mean age in years (SD)	35 (6.4)	36 (6.2)	0.64
Mean adjusted age (SD)	−11 (6.8)	−12 (7.2)	0.73
Mean MMSE score (range)	27.1 (21–30)	28.1 (24–29)	0.40
Gender (# female)	10	7	n.s.

Note: MMSE = Mini-Mental Status Examination

Table 2 Demographic data for the eight presymptomatic (CDR total score = 0) FAD MCs (mutation carriers) and seven non-carriers (NCs)

	FAD MCs ($n = 8$)	FAD NCs ($n = 7$)	*P*-values
Mean age in years (SD)	32 (6.4)	36 (6.6)	0.34
Mean adjusted age (SD)	−13 (6.0)	−12 (7.7)	0.76
Mean MMSE score (range)	28.8 (28–30)	28 (24–29)	0.29
Gender (# female)	7	6	n.s.

Note: MMSE = Mini-Mental Status Examination.

Two-tailed independent sample *t*-tests were performed comparing FA measures, brain volume defined as percent of total intracranial volume, normalized grey and white-matter volumes, cross-sectional area of the columns of the fornix, mean normalized volumes of the right and left hippocampi, MMSE score and adjusted age between preclinical FAD mutation carriers (MCs) and non-carriers (NCs). All *t*-tests were performed twice; once for preclinical subjects and once for presymptomatic subjects.

In order to determine which variables best predicted FAD mutation status in presymptomatic subjects, a logistic regression analysis was performed with mutation status as

the dependent variable. Those variables that differed between mutation carriers and non-carriers with total CDR scores of 0 by *t*-test at the 0.05 significance level were entered as independent variables.

Table 3 MRI variables in the 12 preclinical MCs versus 8 NCs

	FAD MCs ($n=12$)	FAD NCs ($n=8$)	*P*-values
Brain size as percent of intracranial volume	86%	88%	0.125
Gray-matter vol (mm^3)	835 646	844 891	0.752
White-matter vol (mm^3)	776 296	803 328	0.285
Mean *R* and *L* hippocampal volume (mm^3)	3283	3135	0.408
Fornix area, mm^2 (SD)	***16.4 (4.2)***	***20.5 (4.0)***	***0.043***
Mean whole brain WM FA (SD)	***0.30 (0.02)***	***0.32 (0.02)***	***0.045***
FA fornix (SD)	***0.53 (0.09)***	***0.66 (0.11)***	***0.012***
FA R cingulum (SD)	0.49 (0.08)	0.56 (0.07)	0.065
FA L cingulum (SD)	0.49 (0.07)	0.52 (0.08)	0.262
FA R perforant path area (SD)	***0.28 (0.03)***	***0.36 (0.08)***	***0.028***
FA L perforant path area (SD)	***0.29 (0.06)***	***0.36 (0.06)***	***0.027***
FA genu of c.c. (SD)	0.77 (0.06)	0.82 (0.05)	0.089
FA splenium of c.c. (SD)	0.83 (0.09)	0.81 (0.10)	0.551
FA R frontal white matter (SD)	0.51 (0.06)	0.54 (0.07)	0.389
FA L frontal white matter (SD)	***0.50 (0.05)***	***0.56 (0.06)***	***0.024***
FA R CS tract (SD)	0.70 (0.07)	0.69 (0.11)	0.861
FA L CS tract (SD)	0.72 (0.07)	0.70 (0.08)	0.622

Note: FA = fractional anisotropy, R = right, L = left, c.c. = corpus callosum, WM = white matter, CS = corticospinal. *P*-values represent results of two-tailed independent sample *t*-tests. Values that are different at the $P<0.05$ level are shown in bold italics.

To establish what the strongest determinants of fornix FA were, linear regression analyses were performed with fornix FA as the dependent variable and fornix area, normalized white and gray-matter volumes, normalized mean hippocampal volume and FAD mutation status as predictor variables. Data from all 23 subjects were included in the logistic and linear regression analyses. Because of the relatively low numbers of subjects available for this type of study, *P*-values of 0.05 were used throughout without adjustments for multiple comparisons. All analyses were performed using the Statistical Package for the Social Sciences, Version 11.0.2.

Results

Fourteen subjects were FAD MCs and nine were NCs (Fig. 7). Of the 14 FAD MCs, two were demented (CDR scores of 2 and 3). All 23 subjects were female except for one NC and two MCs (1 CDR = 0, 1 CDR = 0.5). One NC was approximately 18 years older than the typical age of diagnosis in her family and therefore was excluded from the *t*-tests comparing preclinical and presymptomatic subjects as she was no longer 'at-risk'. Of the remaining 20 preclinical at-risk subjects, 12 were MCs (CDR = 0.5 in 4, 0 in 8) and 8 were NCs (CDR = 0.5 in 1, 0 in 7). Therefore, 15 subjects (8 MCs and 7 NCs) were presymptomatic (CDR = 0). There were no significant differences in age, adjusted age or MMSE score between the 12 preclinical MCs and 9 NCs (Table 1) nor between the 8 presymptomatic MCs and 7 NCs (Table 2).

There was no significant difference between MCs and NCs in regards to overall brain size, white and gray-matter volumes or mean hippocampal volumes in either preclinical or presymptomatic subjects. Cross-sectional area of the fornix was smaller in MCs in both the preclinical

Table 4 MRI variables in the 8 presymptomatic MCs versus 7 NCs

	FAD MCs ($n=8$)	FAD NCs ($n=7$)	*P*-values
Brain size as percent of intracranial volume	87%	88%	0.257
Gray-matter vol, mm^3	855 311	839 705	0.631
White-matter vol, mm^3	767 920	811 023	0.182
Mean *R* and *L* hippocampal volume, mm^3	3307	3103	0.360
Fornix area, mm^2 (SD)	***16.6 (4.4)***	***21.3 (3.5)***	***0.045***
Mean Whole brain WM FA (SD)	0.30 (0.02)	0.32 (0.02)	0.070
FA fornix (SD)	***0.50 (0.06)***	***0.66 (0.12)***	***0.008***
FA R cingulum (SD)	0.50 (0.09)	0.56 (0.08)	0.195
FA L cingulum (SD)	0.49 (0.07)	0.54 (0.07)	0.195
FA R perforant pathway area (SD)	0.29 (0.03)	0.36 (0.09)	0.067
FA L perforant pathway area (SD)	0.29 (0.07)	0.36 (0.07)	0.076
FA genu of c.c. (SD)	0.77 (0.07)	0.82 (0.05)	0.116
FA splenium of c.c. (SD)	0.84 (0.08)	0.81 (0.10)	0.554
FA R frontal white matter (SD)	0.52 (0.04)	0.53 (0.07)	0.763
FA L frontal white matter (SD)	***0.49 (0.05)***	***0.56 (0.06)***	***0.045***
FA R CS tract (SD)	0.72 (0.05)	0.71 (0.11)	0.780
FA L CS tract (SD)	0.75 (0.06)	0.69 (0.09)	0.201

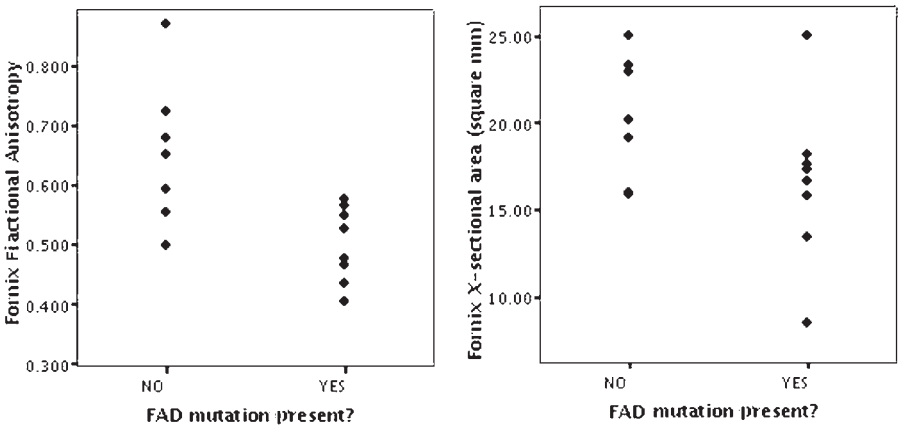

Fig. 8 Scatterplots of the FA (left) and cross-sectional area of the columns of the fornix (right) in 8 FAD MCs and 7 NCs.

(16.4 versus 20.5 mm^2, $P = 0.043$, Table 3) and presymptomatic subjects (16.6 versus 21.3 mm^2, $P = 0.045$, Table 4, Fig. 8). In preclinical and presymptomatic subjects, mean FA values of MCs were numerically lower in all ROIs except for the inferior splenium of the corpus callosum and the right and left corticospinal tracts (Tables 3 and 4). Mean overall FA was statistically lower in the preclinical (0.30 versus 0.32, $P = 0.045$) but not the presymptomatic subjects ($P = 0.070$). FA in the columns of the fornix was also lower in preclinical (0.53 versus 0.66, $P = 0.012$) and presymptomatic (0.50 versus 0.66, $P = 0.008$, Fig. 4) subjects. In the area of the perforant path, FA was lower bilaterally in preclinical MCs (0.28 versus 0.36, $P = 0.028$ on the right side, 0.29 versus 0.36, $P = 0.027$ on the left side). FA was non-significantly decreased in the perforant pathway in presymptomatic MCs (*P*-values of 0.067 on right and 0.076 on the left). FA in MCs was also lower in the white matter of the left frontal lobe (0.50 versus 0.56, $P = 0.024$ for preclinical subjects, 0.49 versus 0.56, $P = 0.045$ for presymptomatic subjects).

In the logistic regression analysis, FA of the fornix was the best predictor of mutation status ($P = 0.005$), followed by left frontal white FA ($P = 0.007$), and cross-sectional area of the fornix ($P = 0.031$). In the linear regression model, white-matter volume was the greatest predictor of fornix FA ($P = 0.002$), followed by hippocampal volume ($P = 0.023$), and FAD mutation status ($P = 0.032$). Cross-sectional area of the fornix ($P = 0.127$) and gray-matter volume ($P = 0.339$) were not significant predictors of fornix FA.

Discussion

In the current study, we found that FA is reduced in specific areas of white matter in persons carrying FAD mutations prior to the development of symptoms of dementia. The global analysis suggests that average whole-brain white-matter FA is reduced in pre-clinical FAD mutation carriers, and the ROI analyses demonstrated that this effect was evident in the fornix and white matter underlying the orbitofrontal region during the presymptomatic stage of the illness. This effect was not present in the early-myelinating regions of splenium of the corpus callosum or the corticospinal tracts at the level of the midbrain. This is consistent with prior studies demonstrating that limbic projections and pathways connecting the frontal lobes are preferentially affected in the course of Alzheimer's disease (Braak and Braak, 1996; Bartzokis *et al.*, 2004). The greatest reduction we found using our methods was in the columns of the fornix and decreased FA in the fornix was a more sensitive measure for predicting FAD mutation status in presymptomatic persons than were cross-sectional area of the fornix, overall brain size, white and grey-matter volumes or hippocampal volumes. Though these measures were not different between preclinical or presymptomatic FAD MCs and NCs, the observation in the linear regression analysis that overall white-matter volume was highly related to fornix FA suggests that low FA in this structure may represent an earlier manifestation of white-matter deterioration than can be detected by comparison of volumes.

Neuronal death occurring secondary to excessive production or decreased degradation of toxic forms of beta-amyloid is the most widely accepted aetiological mechanism for Alzheimer's disease. Nonetheless, multiple studies in both animal models and humans have demonstrated that the integrity of white matter is affected during the course of Alzheimer's disease and indeed can be an early event. Whether myelin pathology is primary or if axonal disruption due to neuronal loss is causative is uncertain but it is clear that changes in white matter occur in Alzheimer's disease and they can be measured using various techniques.

In previous investigations of living subjects, this has been studied by measuring white-matter volumes (Bartzokis *et al.*, 2001), transverse relaxation rates (Bartzokis *et al.*, 2003) and by employing DTI (Medina *et al.*, 2006). The water content of white matter increases as its myelin component decreases in various pathological states. The transverse relaxation rate (R_2) provides an index of the water content

of a tissue with lower values reflecting higher water concentrations. Decreased R_2 values are seen in areas of pathology in demyelinating diseases (Papanikolaou *et al.*, 2004) as well as in normal aging (Bartzokis *et al.*, 2001, 2004), individuals at-risk for Alzheimer's disease (Bartzokis *et al.*, 2006) and Alzheimer's disease (Bartzokis *et al.*, 2003). Prior studies using this technique have demonstrated that R_2 is below normal in the frontal lobe white matter of persons with Alzheimer's disease (Bartzokis *et al.*, 2003) and suggest that R_2 of the frontal lobes and genu of the corpus callosum decreases with age at a faster rate in carriers of the ApoE ε4 allele (Bartzokis *et al.*, 2006). It has been hypothesized that this greater involvement of late-myelinating areas is due to a selective vulnerability of oligodendrocytes in these regions (Bartzokis *et al.*, 2004). Regardless of the underlying cause, our finding of significantly decreased FA in the white matter of the frontal lobe of FAD MCs and trends towards this in the genu of the corpus callosum (despite our small number of subjects) but not in the splenium or corticospinal tract provides convergent evidence for selective involvement of these late-myelinating areas in early Alzheimer's disease.

Neuronal loss is earliest and most severe in the medial temporal lobe in Alzheimer's disease. It might therefore be expected that the most significant alterations in white matter would be found in the tracts connecting this region and other limbic (Callen *et al.*, 2001) and non-limbic brain regions. A previous pathological study demonstrated a 60% loss of neurons in layer II of the entorhinal cortex in persons dying with a CDR score of 0.5 (Gomez-Isla *et al.*, 1996). As the neurons in this layer give rise to the perforant pathway that projects to the hippocampus, one might expect that the FA in this area might decline as result. Indeed, a prior DTI study demonstrated that the intervoxel coherence in the area of the perforant pathway was decreased in persons with MCI compared to controls (Kalus *et al.*, 2006). Using our methods, we were able to detect significant decreases in FA in the area of the perforant pathway bilaterally in preclinical but not presymptomatic FAD MCs. The fornix is the predominant outflow tract of the hippocampus and connects it with the septal nuclei as well as the mamillary bodies in the hypothalamus. FA of the cingulum bundle, another outflow tract of the medial temporal lobe that connects it with the cingulate gyrus, was also reduced, albeit non-significantly so, in presymptomatic MCs. Our finding of decreased FA in the columns of the fornix of persons inheriting but not yet affected by FAD confirms its early involvement in the disease and suggest that FA of the fornix might be a useful index of early disease in sporadic Alzheimer's disease. We know of one prior abstract in which FA of the columns of the fornix was reported to be decreased in persons with Alzheimer's disease (Bozoki *et al.*, 2004).

A prior report found that non-demented persons with an ApoE ε4 allele had decreased FA in the posterior corpus callosum and the left posterior hippocampus compared to controls without this allele (Persson *et al.*, 2006). It is unclear if this represents a consequence of the early changes of Alzheimer's disease of a trait associated with the ApoE ε4 genotype. In our multiple linear regression analysis, we did not find an robust effect of ApoE genotype on fornix FA (data not shown) but our study was likely underpowered to identify such an effect if present (4 of 23 subjects carried an ApoE ε4 allele.

A possible confounder in this study is that atrophy of the fornix in its intraventricular course would also contribute to decreased FA. That is, the smaller the fornix, the more

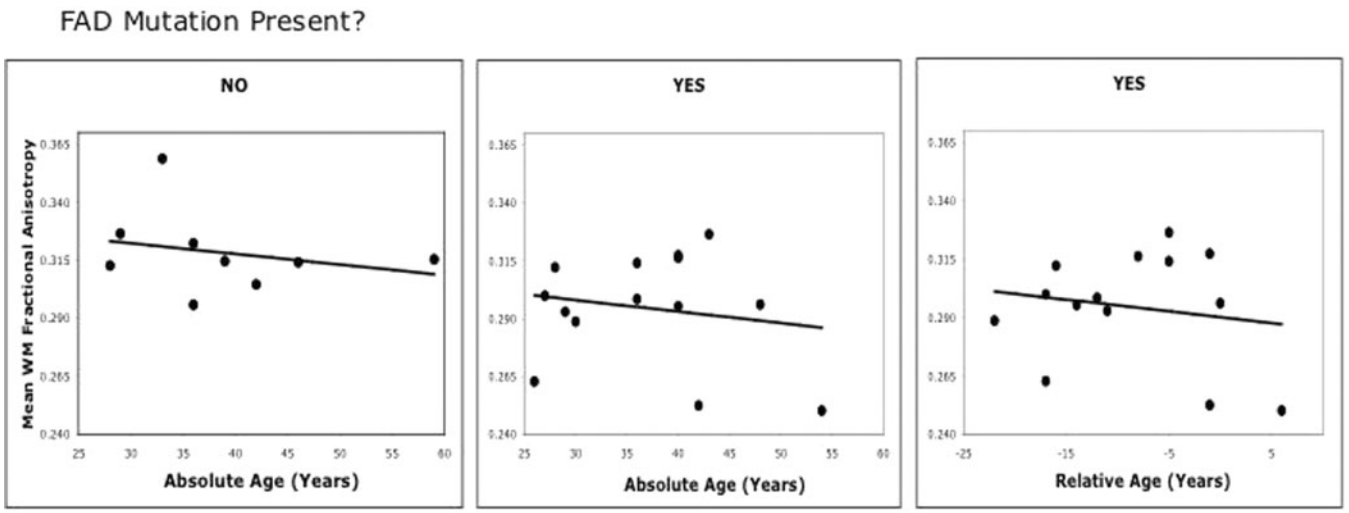

Fig. 9 Scatterplots of mean white-matter FA in FAD NCs and MCs in relation to absolute age (left and middle) and age relative to the family-specific median age of disease diagnosis (adjusted age or 'relative age') in MCs (right).

CSF would be included in a given voxel size (3 mm in our study). Since CSF has an FA near 0, the partial volume effect of increased CSF in the voxel would cause the mean FA within that voxel to be decreased. As the voxels chosen to represent the fornix in our study did not have FAs dramatically lower than those from the parenchymal white matter, we do not feel this effect was pronounced in our study. Also, the regression analyses in our study suggest that cross-sectional area of the fornix influences FA but does not completely explain the decreases seen in FAD MCs. We speculate that the significant drop we see is the composite result of decreased FA within the fornix with a possible smaller contribution from diminished fornix size in these subjects. Replication of our study using higher-resolution DTI would help resolve this question.

An advantage to studying relatively young persons with or at-risk for FAD is the paucity of co-morbid illness (e.g. hypertension) that might contribute to confounding cerebral pathology (e.g. ischaemic changes). None of the subjects in our study had notable non-Alzheimer's cerebral pathology and they thus provide a relatively 'pure' model of the disease. However, there may be limitations to the degree to which the findings of our study of FAD are generalizable to sporadic Alzheimer's disease. Other than age of onset, there are additional clinical (Assini *et al.*, 2003) and pathological (Houlden *et al.*, 2000; Takao *et al.*, 2001) differences between FAD and sporadic Alzheimer's disease. Abnormal white matter may represent a quality of FAD not directly related to the incipient pathology of Alzheimer's disease. Persons carrying FAD mutations may have life-long white-matter abnormalities (a trait) rather than acquired changes (a state) of developing Alzheimer's disease characterized by decreased fractional anisotropy. Though there is a suggestion of accelerated decrease of FA with advancing age in MCs (Fig. 9), the data presented in Fig. 9 are also compatible with even earlier decreases in FA in this population.

Evidence for developmental abnormalities in PS1-related FAD comes from both animal and human studies. Embryos of transgenic mice in which both copies of the PS1 gene have been knocked out have abnormalities of neuronal migration and differentiation characterized by disorganization of the cerebral cortex (Handler *et al.*, 2000). Also, a patient with a PS1 mutation who developed young-onset Alzheimer's disease and came to autopsy was noted to have ectopic neurons in the white matter (Takao *et al.*, 2001). Though we do not know of any such structural abnormalities having been reported in the white matter of persons dying with the FAD mutations included in this study (Mullan *et al.*, 1993; Cochran *et al.*, 2001), such a possibility exists. If present, one might expect that this could account for the differences seen.

If PS1 mutations cause aberrant neuronal migration or other white-matter abnormalities, it would be of interest to know the effect of APP mutations on white-matter integrity as to our knowledge white-matter abnormalities have not been described in pathological specimens of persons dying with APP mutations. Notably, four subjects in the current study were at-risk for the V717I substitution in the APP gene and among them the tendency for MCs to have lower mean white-matter FA was maintained. Unfortunately, due to these small numbers and the necessity to maintain subject anonymity with regard to mutation status little more can be said or concluded about this.

Among persons with the A431E substitution in the PSEN1 gene, many develop significant spastic tetraparesis as the dementia progresses (Murrell *et al.*, 2006). In pathological studies, tetraparesis occurring in FAD has been related to disproportionate involvement of the motor cortex with amyloid pathology with presumptive consequent degeneration of the corticospinal tracts. None of the 11 subjects in our study at-risk for this mutation had significant para- or tetraparesis but it is notable that one such MC who had a CDR score of 0.5 was hyperreflexic and had relatively low FA of the corticospinal tract in the cerebral peduncle (data not shown). This suggests that DTI may have utility in detecting and possibly in predicting this complication.

Our data indicate that loss of white-matter integrity, as indexed by FA acquired through DTI, is an early feature in FAD. Furthermore, this loss is somewhat selective, disproportionately affecting tracts that connect limbic structures and the frontal lobes. Though there are limitations to our study regarding the resolution of the DTI technique employed and the ability to generalize from FAD to the more common form of late-onset Alzheimer's disease, we feel that further investigations of early changes in white matter, particularly of the FA of the columns of the fornix, are merited as potential indicators or even predictors of Alzheimer's disease status.

Acknowledgements

This study was supported by PHS K08 AG-22228, California DHS #04-35522, M01-RR00865, General Clinical Research Centers Program and the Shirley and Jack Goldberg Trust. Further support for this study came from Alzheimer's Disease Research Center Grant AG-16570 from the National Institute on Aging, an Alzheimer's Disease Research Center of California grant, and the Sidell Kagan Foundation.

References

Assini A, Terreni L, Borghi R, Giliberto L, Piccini A, Loqui D, et al. Pure spastic paraparesis associated with a novel presenilin 1 R278K mutation. Neurology 2003; 60: 150.

Bartzokis G. Age-related myelin breakdown: a developmental model of cognitive decline and Alzheimer's disease. Neurobiol Aging 2004; 25: 5–18 author reply 49–62.

Bartzokis G, Beckson M, Lu PH, Nuechterlein KH, Edwards N, Mintz J. Age-related changes in frontal and temporal lobe volumes in men: a magnetic resonance imaging study. Arch Gen Psychiatry 2001; 58: 461–5.

Bartzokis G, Cummings JL, Sultzer D, Henderson VW, Nuechterlein KH, Mintz J. White matter structural integrity in healthy aging adults and patients with Alzheimer disease: a magnetic resonance imaging study. Arch Neurol 2003; 60: 393–8.

Bartzokis G, Lu PH, Geschwind DH, Edwards N, Mintz J, Cummings JL. Apolipoprotein E genotype and age-related myelin breakdown in healthy individuals: implications for cognitive decline and dementia. Arch Gen Psychiatry 2006; 63: 63–72.

Bartzokis G, Sultzer D, Lu PH, Nuechterlein KH, Mintz J, Cummings JL. Heterogeneous age-related breakdown of white matter structural integrity: implications for cortical "disconnection" in aging and Alzheimer's disease. Neurobiol Aging 2004; 25: 843–51.

Basser PJ, Mattiello J, LeBihan D. MR diffusion tensor spectroscopy and imaging. Biophys J 1994; 66: 259–67.

Behrens TE, Woolrich MW, Jenkinson M, Johansen-Berg H, Nunes RG, Clare S, et al. Characterization and propagation of uncertainty in diffusion-weighted MR imaging. Magn Reson Med 2003; 50: 1077–88.

Bozoki A, Delano M, Huang J, Potchen M. Diffusion tensor imaging of the fornix in Alzheimer's disease. Neurology 2004; 62: A126.

Bozzali M, Falini A, Franceschi M, Cercignani M, Zuffi M, Scotti G, et al. White matter damage in Alzheimer's disease assessed in vivo using diffusion tensor magnetic resonance imaging. J Neurol Neurosurg Psychiatry 2002; 72: 742–6.

Braak H, Braak E. Development of Alzheimer-related neurofibrillary changes in the neocortex inversely recapitulates cortical myelogenesis. Acta Neuropathol (Berl) 1996; 92: 197–201.

Callen DJ, Black SE, Gao F, Caldwell CB, Szalai JP. Beyond the hippocampus: MRI volumetry confirms widespread limbic atrophy in AD. Neurology 2001; 57: 1669–74.

Chia LS, Thompson JE, Moscarello MA. X-ray diffraction evidence for myelin disorder in brain from humans with Alzheimer's disease. Biochim Biophys Acta 1984; 775: 308–12.

Cochran EJ, Murrell JR, Fox J, Ringman J, Ghetti B. A novel mutation in the Presenilin-1 gene (A431E) associated with early-onset Alzheimer's disease. J Neuropathol Exp Neurol 2001; 60: 544.

Englund E, Brun A, Alling C. White matter changes in dementia of Alzheimer's type. Biochemical and neuropathological correlates. Brain 1988; 111 (Pt 6): 1425–39.

Fox NC, Kennedy AM, Harvey RJ, Lantos PL, Roques PK, Collinge J, et al. Clinicopathological features of familial Alzheimer's disease associated with the M139V mutation in the presenilin 1 gene. Pedigree but not mutation specific age at onset provides evidence for a further genetic factor. Brain 1997; 120: 491–501.

Gomez-Isla T, Price JL, McKeel DW Jr, Morris JC, Growdon JH, Hyman BT. Profound loss of layer II entorhinal cortex neurons occurs in very mild Alzheimer's disease. J Neurosci 1996; 16: 4491–500.

Handler M, Yang X, Shen J. Presenilin-1 regulates neuronal differentiation during neurogenesis. Development 2000; 127: 2593–606.

Houlden H, Baker M, McGowan E, Lewis P, Hutton M, Crook R, et al. Variant Alzheimer's disease with spastic paraparesis and cotton wool plaques is caused by PS-1 mutations that lead to exceptionally high amyloid-beta concentrations. Ann Neurol 2000; 48: 806–8.

Jenkinson M, Smith S. A global optimisation method for robust affine registration of brain images. Med Image Anal 2001; 5: 143–56.

Kalus P, Slotboom J, Gallinat J, Mahlberg R, Cattapan-Ludewig K, Wiest R, et al. Examining the gateway to the limbic system with diffusion tensor imaging: the perforant pathway in dementia. Neuroimage 2006; 30: 713–20.

Kantarci K, Petersen RC, Boeve BF, Knopman DS, Weigand SD, O'Brien PC, et al. DWI predicts future progression to Alzheimer disease in amnestic mild cognitive impairment. Neurology 2005; 64: 902–4.

Medina D, DeToledo-Morrell L, Urresta F, Gabrieli JD, Moseley M, Fleischman D, et al. White matter changes in mild cognitive impairment and AD: a diffusion tensor imaging study. Neurobiol Aging 2006; 27: 663–72.

Mullan M, Tsuji S, Miki T, Katsuya T, Naruse S, Kaneko K, et al. Clinical comparison of Alzheimer's disease in pedigrees with the codon 717 Val—>Ile mutation in the amyloid precursor protein gene. Neurobiol Aging 1993; 14: 407–19.

Murrell J, Ghetti B, Cochran E, Macias-Islas MA, Medina L, Varpetian A, et al. The A431E mutation in PSEN1 causing Familial Alzheimer's Disease originating in Jalisco State, Mexico: an additional fifteen families. Neurogenetics 2006; 7: 277–9.

Pak K, Chan SL, Mattson MP. Presenilin-1 mutation sensitizes oligodendrocytes to glutamate and amyloid toxicities, and exacerbates white matter damage and memory impairment in mice. Neuromolecular Med 2003; 3: 53–64.

Pantel J, O'Leary DS, Cretsinger K, Bockholt HJ, Keefe H, Magnotta VA, et al. A new method for the in vivo volumetric measurement of the human hippocampus with high neuroanatomical accuracy. Hippocampus 2000; 10: 752–8.

Papanikolaou N, Papadaki E, Karampekios S, Spilioti M, Maris T, Prassopoulos P, et al. T2 relaxation time analysis in patients with multiple sclerosis: correlation with magnetization transfer ratio. Eur Radiol 2004; 14: 115–22.

Persson J, Lind J, Larsson A, Ingvar M, Cruts M, Van Broeckhoven C, et al. Altered brain white matter integrity in healthy carriers of the APOE epsilon4 allele: a risk for AD? Neurology 2006; 66: 1029–33.

Rose SE, McMahon KL, Janke AL, O'Dowd B, de Zubicaray G, Strudwick MW, et al. Diffusion indices on magnetic resonance imaging and neuropsychological performance in amnestic mild cognitive impairment. J Neurol Neurosurg Psychiatry 2006; 77: 1122–8.

Smith SM. Fast robust automated brain extraction. Hum Brain Mapp 2002; 17: 143–55.

Smith SM, Jenkinson M, Woolrich MW, Beckmann CF, Behrens TE, Johansen-Berg H, et al. Advances in functional and structural MR image analysis and implementation as FSL. Neuroimage 2004; 23 (Suppl 1): S208–19.

Smith SM, Zhang Y, Jenkinson M, Chen J, Matthews PM, Federico A, et al. Accurate, robust, and automated longitudinal and cross-sectional brain change analysis. Neuroimage 2002; 17: 479–89.

Takao M, Ghetti B, Murrell JR, Unverzagt FW, Giaccone G, Tagliavini F, et al. Ectopic white matter neurons, a developmental abnormality that may be caused by the PSEN1 S169L mutation in a case of familial AD with myoclonus and seizures. J Neuropathol Exp Neurol 2001; 60: 1137–52.

Tang MX, Stern Y, Marder K, Bell K, Gurland B, Lantigua R, et al. The APOE-epsilon4 allele and the risk of Alzheimer disease among African Americans, whites, and Hispanics. JAMA 1998; 279: 751–5.

Terry RD, Gonatas NK, Weiss M. Ultrastructural studies in Alzheimer's Presenile dementia. Am J Pathol 1964; 44: 269–97.

Wirths O, Weis J, Szczygielski J, Multhaup G, Bayer TA. Axonopathy in an APP/PS1 transgenic mouse model of Alzheimer's disease. Acta Neuropathol (Berl) 2006; 111: 312–9.

Zhang Y, Brady M, Smith S. Segmentation of brain MR images through a hidden Markov random field model and the expectation-maximization algorithm. IEEE Trans Med Imaging 2001; 20: 45–57.